INTERNATIONAL JOURNAL OF OPTIMIZATION IN CIVIL ENGINEERING
Int. J. Optim. Civil Eng., 2014; 4(1):1-26

NEURAL NETWORK-BASED RELIABILITY ASSESSMENT OF OPTIMALLY SEISMIC DESIGNED MOMENT FRAMES

S. Gholizadeh[*, †], V. Aligholizadeh and M. Mohammadi
Department of Civil Engineering, Urmia University, Urmia, Iran

ABSTRACT

In the present study, the reliability assessment of performance-based optimally seismic designed reinforced concrete (RC) and steel moment frames is investigated. In order to achieve this task, an efficient methodology is proposed by integrating Monte Carlo simulation (MCS) and neural networks (NN). Two NN models including radial basis function (RBF) and back propagation (BP) models are examined in this study. In the proposed methodology, MCS is used to estimate the total exceedence probability associated with immediate occupancy (IO), life safety (LS) and collapse prevention (CP) performance levels. To reduce the computational burden of MCS process, the required nonlinear responses of the generated structures are predicted by RBF and BP models. The numerical results imply the superiority of BP to RBF in prediction of structural responses associated with performance levels. Finally, the obtained results demonstrate the high efficiency of the proposed methodology for reliability assessment of RC and steel frame structures.

Received: 10 December 2013; Accepted: 20 February 2014

KEY WORDS: Seismic reliability, performance-based design, structural optimization, Monte Carol simulation, neural network

1. INTRODUCTION

Performance-based design (PBD) [1-3] of structures subject to sever ground motions is an efficient design process and many researchers and engineers have proposed various methodologies, which incorporated PBD concepts and criteria, to improve structural performance. In essence, PBD process is based on the principle that a structure should meet performance levels according to a set of specified reliabilities over its service life. The PBD

[*]Corresponding author: S. Gholizadeh, Department of Civil Engineering, Urmia University, Urmia, Iran
[†]E-mail address: s.gholizadeh@urmia.ac.ir

approach aims to present structural configurations with a predictable and reliable performance level which highly depends on structural seismic responses and capacity that both of these parameters are inherently uncertain. In addition, material properties and characteristics associated with ground motions are also uncertain parameters. Theory and methods for structural reliability assessment have been developed substantially in the last few years and they are actually useful tools for evaluating rationally the safety of structures against the existing uncertainties. Thus, the reliability theory and PBD approach should be simultaneously utilized to design reliable structures for earthquake loadings.

During the last years, some computational strategies have been proposed for seismic reliability assessment of reinforced concrete (RC) and steel structures. Several researchers [4–6] have followed different methods and strategies in developing fragility curves for RC structures. Moller *et. al*. [7–8] proposed a methodology with variable uncertainties for seismic vulnerability of RC frames. In this approach, seismic vulnerability was defined as the conditional probability of exceeding different limit states within a performance requirement, given by a hazard level. They used neural network techniques to evaluate the required structural responses. In the most recent work, Khatibinia *et. al*. [9] proposed a meta-model to reduce the computational cost in seismic reliability assessment of existing RC structures considering soil-structure interaction (SSI) effects. Their proposed meta-model was designed by combining weighted least squares support vector machine (WLS-SVM) and a wavelet kernel function. Their study showed that SSI has the significant influence on the seismic reliability assessment of structures. In the case of steel structures, Lagaros *et. al*. [10] proposed NN-based strategies for solving reliability-robust design optimization problems. They used standard BP model for predicting structural responses during the optimization process.

Nonlinear structural analysis by finite element method (FEM) is a time consuming process. Consequently, the required computational cost will be expensive when the nonlinear structural responses are required for seismic reliability assessment of the structure using MSC. The MCS method requires a large number of structural analyses in order to obtain an acceptable confidence within probabilities of the order close to 10^{-4} –10^{-6}. For such results, the number of analyses that will achieve a 95% likelihood for actual probability must be between 1.6×10^{6} and 1.6×10^{9} [11]. One of the best candidates to reduce the computational burden of evaluating nonlinear structural responses required for performing seismic reliability assessment is soft computing-based approximation tools: neural network (NN) and support vector machines (SVM). A comprehensive review of NNs and SVMs applied for reliability assessment of structural systems has been presented in [9].

In the present study, the bat algorithm (BA) [12] are employed to find performance-based seismic optimum deign of two RC frames and two steel frames. The BA is a newly developed meta-heuristic optimization algorithm based on the echolocation behavior of bats. The capability of echolocation of bats is fascinating, as these bats can find their prey and discriminate different types of insects even in complete darkness. The superiority of BA to some popular meta-heuristic algorithms such as genetic algorithm (GA) and particle swarm optimization (PSO) for solving engineering optimization problems have been demonstrated [13] and thus in this paper BA is utilized to implement optimization process. In order to assess reliability of the optimally seismic designed structures for existing

uncertainties a combination of MCS method and NN models is employed. Radial basis function (RBF) and back propagation (BP) neural networks, as two popular networks, are employed to predict the seismic responses of the frame structures in the framework of MCS. The numerical results indicate that the BP model in conjunction with MCS method provides a powerful computational tool for reliability assessment of RC and steel frames.

2. OPTIMAL SEISMIC DESIGN

Many studies have shown that structures designed by modern seismic code procedures are expected to undergo large cyclic deformations in the inelastic range when subjected to severe earthquake ground motions. Nevertheless, most seismic design codes are still based on elastic methods using equivalent static lateral design forces. This procedure can result in unpredictable and poor response during severe ground motions with inelastic activity unevenly distributed among structural members. To solve this problem, performance-based design (PBD) procedure was developed. PBD procedures allow engineers to determine explicitly performance of structures for a special seismic hazard level. PBD enables designers to design structures having predictable and reliable performance against seismic loadings. The designs obtained by PBD approach should meet performance objectives. A performance objective is defined as a given level of performance for a specific hazard level. To define a performance objective, at first the level of structural performance should be selected and then the corresponding seismic hazard level should be determined. In the present work, immediate occupancy (IO), life safety (LS) and collapse prevention (CP) performance levels are considered according to FEMA-356 [1]. Each objective corresponds to a given probability of being exceed during 50 years. A usual assumption [14] is that the IO, LS and CP performance levels correspond respectively to a 20%, 10% and 2% probability of exceedance in 50 year period. In this study, the mentioned hazard levels are considered.

2.1 Nonlinear pushover analysis

The estimation of demands can be accomplished using a variety of available procedures. Using the nonlinear static procedure, the inelastic behavior of the structure as a whole can be captured by a static pushover curve. The pushover curve gives an accurate description of the structural behavior, compared to the dynamic analysis, at least for a structure that has a low number of participating modes. The advantage in utilizing a pushover analysis relies in the fact that it can be used in most practical cases. On the other hand, dynamic inelastic time history analyses are often difficult to implement. The practical objective of inelastic seismic analysis procedures is to predict the expected behavior of the structure in future earthquake shaking. This has become increasingly important with the emergence of performance-based engineering (PBE) as a technique for seismic evaluation and design [15]. Among the various methods of static nonlinear pushover analyses, the displacement coefficient method [1] is adopted to evaluate the seismic demands on building frameworks under equivalent static earthquake loading. In this method the structure is pushed with a specific distribution of the lateral loads until the target displacement is reached. The target displacement can be

obtained from the FEMA-356 as follows:

$$\delta_t = C_0 C_1 C_2 C_3 S_a \frac{T_e^2}{4\pi^2} g \tag{1}$$

where C_0 relates the spectral displacement to the likely building roof displacement; C_1 relates the expected maximum inelastic displacements to the displacements calculated for linear elastic response; C_2 represents the effect of the hysteresis shape on the maximum displacement response and C_3 accounts for P-D effects. T_e is the effective fundamental period of the building in the direction under consideration; S_a is the response spectrum acceleration corresponding to the T_e.

In this work, the OPENSEES [16] platform is utilized to conduct the pushover analyses.

2.2 Problem formulation

In a sizing structural optimization problem, the aim is usually to minimize the weight or cost of the structure under some behavioural constraints. For a frame structure consisting of *ne* members that are collected in *n* design groups, if the variables associated with each design group are selected from a given database of sections, a discrete optimization problem can be formulated as follows:

$$\begin{aligned} &\text{Minimize } f(\mathrm{X}) \\ &\text{Subject to: } g_i(X) \le 0 \quad i = 1,2,\cdots,\mathrm{ng} \\ &X = \{x_1 \quad x_2 \quad \ldots \quad x_j \quad \ldots \quad x_n\}^{\mathrm{T}} \end{aligned} \tag{2}$$

where x_j is an integer value expressing the sequence numbers of sections assigned to *j*th group; f represents the objective function of the frame; $g_i(X)$ is the *i*th behavioral constraint; *ng* is the number of constraints.

Objective function for a RC frame, f_{R}, is usually taken as the cost of structure and can be defined as follows [17]:

$$\begin{aligned} f_{\mathrm{R}} = &\sum_{i=1}^{nb} \left(\mathrm{C_C b}_{b,i} \mathrm{h}_{b,i} + C_S \, \mathrm{A}_{\mathrm{S},b,i} + C_F (\mathrm{b}_{b,i} + 2\mathrm{h}_{b,i}) \right) \mathrm{L_i} + \\ &\sum_{j=1}^{nc} \left(\mathrm{C_C b}_{c,j} \mathrm{h}_{c,j} + C_S \, \mathrm{A}_{\mathrm{S},c,j} + 2C_F (\mathrm{b}_{c,j} + \mathrm{h}_{c,j}) \right) \mathrm{H_j} \end{aligned} \tag{3}$$

where *nb* is the number of beams; $b_{b,i}$, $h_{b,i}$, L_i and $A_{S,b,i}$ are the *i*th beam width, depth, length and area of the steel reinforcement, respectively; *nc* is the number of columns; $b_{c,j}$, $h_{c,j}$, H_j and $A_{S,c,j}$ are the *j*th column width, depth, length and area of the steel reinforcement, respectively; C_C, C_S and C_F are the unit cost of concrete, steel and framework, respectively. As mentioned in [17], in the present work the following unit costs are also considered: C_C=105 \$/m^3, C_S=7065 \$/ m^3, C_F=92 \$/ m^2.

In the case of a steel frame, the weight of structure is usually considered as the objective

function, f_S, and it can be defined as follows [18]:

$$f_S = \sum_{i=1}^{n} \rho_i A_i \sum_{j=1}^{nm} L_j \tag{4}$$

where ρ_i and A_i are weight of unit volume and cross-sectional area of the ith group section, respectively; nm is the number of elements collected in the ith group; L_j is the length of the jth element in the ith group.

In this study, the constraints of the optimization problem are handled using the concept of exterior penalty functions method (EPFM) [19]. In this case, the pseudo unconstrained objective function is expressed as follows:

$$\Phi(X, r_p) = f(X).\left(1 + r_p \sum_{i=1}^{nc} \left(\max\{0, g_i(X)\}\right)^2\right) \tag{5}$$

where Φ and r_p are the pseudo objective function and positive penalty parameter, respectively.

In this work, two types of constraints are checked during the optimization process. The first type includes the checks of each structural element for gravity loads. In this case, the following load combination is considered:

$$Q_{G1} = 1.2Q_D + 1.6Q_L \tag{6}$$

where Q_D and Q_L are dead and live loads, respectively.

Each structural element of RC and steel frames should satisfy the constraints specified respectively by ACI 318-08 [20] and LRFD-AISC [21] codes for the non-seismic load combination.

If the first type constraints are not satisfied then the candidate design is rejected, else a nonlinear pushover analysis is performed in order to estimate the maximum inter-story drift ratios at various performance levels. In nonlinear static pushover analysis, the lateral load distribution in the height of the frame is defined as follows [1]:

$$P_s = V_b\left(\frac{G_s H_s^k}{\sum_{m=1}^{ns} G_m H_m^k}\right) \tag{7}$$

where P_s = lateral load applied at story s; V_b = base shear; H_s, H_m = height from the base of the building to stories s and m, respectively; G_s, G_m = seismic weight for story levels s and m, respectively; k = 2 and this means that the lateral load pattern is parabolic.

The following component gravity force is considered for combination with the seismic loads [1]:

$$Q_{G2} = 1.1(Q_D + Q_L) \tag{8}$$

In this study, the lateral inter-story drift ratios are considered as the acceptance criteria. The inter-story drift ratio constraints at various performance levels can be expressed as:

$$g_i^l(X) = \frac{\theta_i^l}{\theta_{all}^l} - 1 \le 0 \quad , \quad l = \text{IO; LS; CP}, \quad i = 1,2,...,ns \tag{9}$$

where θ_i^l and θ_{all}^l are respectively the *i*th story drift and its allowable value associated with *l*th performance level; *ns* is the number of stories.

In order to find performance-based seismic optimum deign of frames BA is employed. The basic concepts of BA are defined as follows.

2.3 Bat algorithm

The BA meta-heuristic is inspired from the echolocation behaviour of microbats [22]. The echolocation characteristics of microbats in BA are idealized as the following three rules [13]. The first rule is that all bats use echolocation to sense distance, and they also know the difference between prey and background barriers in some magical way. As the second rule, bats randomly fly with velocity V_i at position X_i with a fixed frequency $f_{\min}$, varying wavelength and loudness Ω^0 to search for prey. They can adjust the frequency of their emitted pulses and adjust the rate of pulse emission $r \in [0,1]$, depending on the proximity of their target. The third rule says that although the loudness can vary in many ways, it is assumed that the loudness varies from a large and positive Ω^0 to a minimum constant value $\Omega_{\min}$.

The position and velocity of each bat should be updated in the design space. As optimization of RC and steel frames using the section databases is a discrete optimization problem, the following equations are employed for updating position and velocity of *i*th bat:

$$f_i = f_{\min} + (f_{\max} - f_{\min})u_i \tag{10}$$

$$V_i^{k+1} = \text{round}\left(V_i^k + (X_i^k - X^*)\, f_i\right) \tag{11}$$

$$X_i^{k+1} = X_i^k + V_i^{k+1} \tag{12}$$

where $f_{\min}$ and $f_{\max}$ are the lower and upper bounds imposed for the frequency range of bats. In this study, $f_{\min}$=0.0 and $f_{\max}$=1.5 are used; $u_i \in [0,1]$ is a vector containing uniformly distribution random numbers; X^* is the current global best solution;

A local search is implemented on a randomly selected bat from the current population as:

$$X^{k+1} = X^k + \text{round}\,(\varepsilon_j\, \Omega^{k+1}) \tag{13}$$

where ε_j is a uniform random number in the range of [-1, 1] selected for each design variable of the selected bat. Ω^{k+1} is the average loudness of all the bats at the current iteration.

The loudness Ω_i and the rate r_i of pulse emission have to be updated accordingly as the

iterations proceed. As the loudness usually decreases once a bat has found its prey, while the rate of pulse emission increases, the loudness can be chosen as any value of convenience. In this work, $\Omega^0 = 1$and $\Omega_{\min} = 0$ also, $r^0 = 0$ and $r_{\max} = 1$.

$$\Omega_i^{k+1} = \alpha\, \Omega_i^k \tag{14}$$

$$r_i^{k+1} = r_i^0 \,(1 - \mathrm{e}^{-\gamma.k}) \tag{15}$$

where α and γ are constants. In this study, $\alpha = 0.5$, and $\gamma = 0.5$.

3. SEISMIC RELIABILITY ASSESSMENT

Deterministic structural optimization without considering the uncertainties in structural capacity and seismic demands results in an unreliable design and cannot balance both cost and safety. The structural seismic responses can be affected by many uncertain variables. Material properties and earthquake loading are considered as intervening uncertain variables in this study. Therefore, the main aim of the present paper is to assess the seismic reliability of optimally seismic designed RC and steel frames considering the mentioned sources of uncertainties. To achieve this purpose, nonlinear pushover analysis of the structures is implemented to obtain the structural seismic responses. The limit state functions associated with each performance level are calculated using the structural seismic responses. Then, the non-performance probability corresponding to each performance level is evaluated. MCS is a powerful tool, simple to implement and capable of solving a broad range of reliability problems. However, its use for evaluation of very low probabilities of failure implies a great number of structural analyses which can become excessively time consuming especially when the nonlinear analysis is involved. To reduce the computational burden of the MCS-based reliability assessment process, RBF and BP NN models are employed to predict the required nonlinear responses of the structures at IO, LS and CP performance levels. The proposed methodology provides the possibility of reproducing structural behavior for performance evaluation at a trivial computational cost. In order to obtain seismic reliability assessment using the proposed methodology, random samples are generated and used to train and test the RBF and BP NN models. Random combinations of intervening variables and the corresponding desired structural seismic responses are respectively considered as input and outputs of the NN models.

3.1 Input and output vectors

For structural elements of RC frames, Kent–Scott–Park model [23] is used as the confined and unconfined concrete constitutive model. The concrete of cover and core in cross-section of the columns is considered as unconfined and confined, respectively. As shown in Figure 1(a) f_c, f_u, ε_0 and ε_u are the constitutive parameters of this model representing respectively concrete peak strength in compression, residual strength, strain at peak strength, and ultimate compressive strain. Constitutive behavior of the reinforcing steel shown in Figure

1(b) is based on using the one-dimensional plasticity model with linear hardening. The material parameters of E, f_y and H which are respectively Young's modulus, yield strength, and hardening modulus define the plasticity model. In this study, the above constitutive parameters f_c, E and f_y are considered as the random parameters. For structural elements of steel frames, the constitutive behavior of Figure 1(b) is employed considering E and f_y as the random parameters. Beams and columns of the RC and steel moment frames are modeled using force-based nonlinear beam-column element on the OPENSEES platform that considers the spread of plasticity along the element's length.

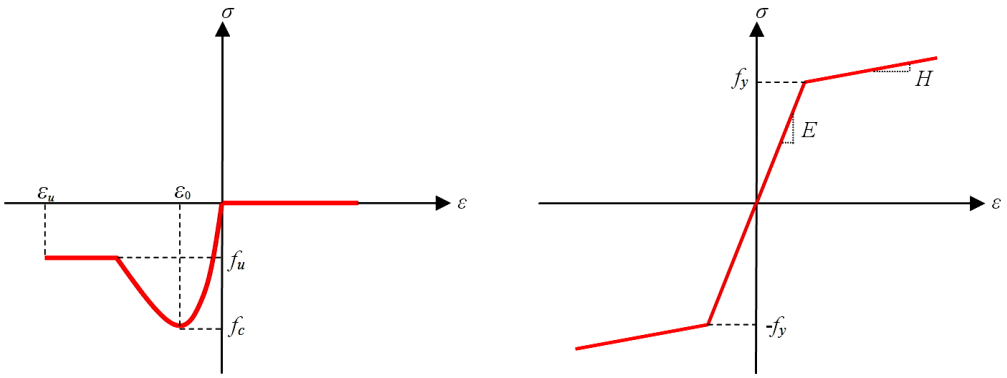

(a) (b)

Figure 1. Material constitutive behavior (a) concrete, (b) steel

In this study, response spectrum acceleration S_a associated with the mentioned triple hazard levels are considered as the random parameters termed here as S_a^{IO}, S_a^{LS} and S_a^{CP}. Therefore, the random variables vector for RC and Steel frames which are employed as the input vector of the NN models can be represented as follows:

$$I_{\mathrm{NN,R}} = \{ f_c \quad E \quad f_y \quad S_a^{\mathrm{IO}} \quad S_a^{\mathrm{LS}} \quad S_a^{\mathrm{CP}} \}^{\mathrm{T}} \tag{16}$$

$$I_{\mathrm{NN,S}} = \{ E \quad f_y \quad S_a^{\mathrm{IO}} \quad S_a^{\mathrm{LS}} \quad S_a^{\mathrm{CP}} \}^{\mathrm{T}} \tag{17}$$

where $I_{\mathrm{NN,R}}$ and $I_{\mathrm{NN,S}}$ are input vectors of NN models for RC and steel frames, respectively.

It should be noted that in a structure including n design groups, a set of random constitutive parameters is considered for each design group. In this case, constitutive parameters f_c, E and f_y are vectors defined as follows:

$$f_c = \{ f_{c1} \quad f_{c2} \quad \cdots \quad f_{ci} \quad \cdots \quad f_{cn} \}^{\mathrm{T}} \tag{18}$$

$$E = \{ E_1 \quad E_2 \quad \cdots \quad E_i \quad \cdots \quad E_n \}^{\mathrm{T}} \tag{19}$$

$$f_y = \{ f_{y1} \quad f_{y2} \quad \cdots \quad f_{yi} \quad \cdots \quad f_{yn} \}^{\mathrm{T}} \tag{20}$$

For seismic reliability assessment, maximum inter-story drift ratios at IO, LS and CP performance levels are selected as the structural seismic responses. Thus, for both RC and steel frames the output vector of the NN models, O_{NN}, is as follows:

$$O_{NN} = \{\theta_{max}^{IO} \quad \theta_{max}^{LS} \quad \theta_{max}^{CP}\}^{T} \tag{21}$$

3.2 Monte carlo simulation

A reliability problem is normally formulated using a limit state function. Limit state function for each performance level is defined using capacity and demand as follows:

$$G(Z) = R_{LIM} - R(Z) \tag{22}$$

where G is a limit state function; Z is the vector of random variables defined for RC and steel frames by Eqs. (16) to (20); R_{LIM} is the limiting value for a seismic response $R(Z)$.

In similar studies such as [7-9] the limiting capacities R_{LIM} were also considered random. In the present study, these parameters for RC and steel frames are considered deterministic. As in the present work only the maximum inter-story drift ratios at the performance levels are selected as the structural seismic responses, the limit state functions considered for the three performance levels are as follows:

$$\textit{Immediate Occupancy}: \quad G_{IO}(Z) = \theta_{LIM}^{IO} - \theta_{max}^{IO}(Z) \tag{23}$$

$$\textit{Life Safety}: \quad G_{LS}(Z) = \theta_{LIM}^{LS} - \theta_{max}^{LS}(Z) \tag{24}$$

$$\textit{Collapse Prevention}: \quad G_{CP}(Z) = \theta_{LIM}^{CP} - \theta_{max}^{CP}(Z) \tag{25}$$

where θ_{LIM}^{IO}, θ_{LIM}^{LS} and θ_{LIM}^{CP} are the limiting values for maximum inter-story drift seismic responses at the IO, LS and CP performance levels, respectively.

The non-performance probability, P_f, is defined as a function of the limit state functions corresponding to a given performance level. Estimation of the non-performance probability in the time-invariant domain requires the evaluation of the multiple integral over the failure domain, $G(Z) < 0$, as follows [9]:

$$P_f = \iint_{G(Z)} \cdots \int F_Z(Z)\mathrm{d}Z \tag{26}$$

where $F_Z(Z)$ is the joint probability density function of Z.

The total exceedence probability, Pf_E, for each performance level is defined as a series system when one of the limit state functions fails:

$$Pf_E = P\left(\bigcup_{i=1}^{n_l}\{G_i(Z) \le 0\}\right) \tag{27}$$

where n_l is the number of the limit state functions for each performance level.

As in the present work only one limit state function is defined for each performance level, Eq. (27) can be rewritten as follows:

$$Pf_{E,l} = P\left(G_l(Z) \le 0\right) \ , \quad l = \text{IO, LS, CP} \tag{28}$$

Computation of total exceedence probability, $Pf_{E,l}$, requires integration of a multi-normal distribution function [9]. This integral can be estimated by the MCS method. In this study, the MCS method is utilized simultaneously for all limit state functions of the performance levels. The MCS method allows the determination of an estimate of $Pf_{E,l}$, given by

$$Pf_{E,l} = \frac{1}{N}\sum_{i=1}^{N} I_{l,i}(Z) \ , \quad l = \text{IO, LS, CP} \tag{29}$$

$$I_l(Z) = \begin{cases} 1 & \text{if } G_l(Z) \le 0 \\ 0 & \text{if } G_l(Z) > 0 \end{cases} , \quad l = \text{IO, LS, CP} \tag{30}$$

where N is the number of independent samples generated based on the probability distribution for each random variable for implementation MCS.

Implementation of the MCS requires a large number of structural nonlinear pushover analyses. The MCS is a time consuming process because of high computational cost of pushover analysis. To reduce the computational burden of MCS, the required structural seismic responses are predicted by NN models.

4. NEURAL NETWORKS

The principal advantage of a properly trained NN is that it requires a trivial computational burden to produce an approximate solution. Such approximations appear to be valuable in situations where the actual response computations are intensive in terms of computing time and a quick estimation is required. For such problems a NN model is trained utilizing information generated from a number of properly selected analyses. The data from these analyses are processed in order to obtain the necessary input and target pairs, which are subsequently used to train the network [24]. In the present paper, two well known and popular NN models are employed: Radial basis function (RBF) and Back-propagation (BP).

4.1 RBF model

RBF neural networks due to their fast training, generality and simplicity are popular. They are two layers feed forward networks. The hidden layer consists of RBF neurons with Gaussian activation functions. The outputs of RBF neurons have significant responses to the inputs only over a range of values called the receptive field. The radius of the receptive field allows the sensitivity of the RBF neurons to be adjusted. During the training, the receptive

field radius of RBF neurons is such determined as the neurons could cover the input space properly. The output layer neurons produce the linear weighted summation of hidden layer neurons responses. To train the hidden layer of RBF networks no training is accomplished and the transpose of training input matrix is taken as the layer weight matrix [25].

$$W_1^{\mathrm{RBF}} = \Lambda^{\mathrm{T}} \tag{31}$$

where, W_1^{RBF} and Λ^{T} are input layer weight and training input matrices, respectively.

In order to adjust output layer weights, a supervised training algorithm is employed. The output layer weight matrix is calculated from the following equation:

$$W_2^{RBF} = \Delta^{-1} T \tag{32}$$

where T is target matrix, Δ is the outputs of the hidden layer and W_2^{RBF} is the output layer weight matrix.

4.2 BP model

Standard BP [26] is a gradient descent optimization algorithm, which adjusts the weights in the steepest descent direction according to the following equation:

$$W_{k+1}^{\mathrm{BP}} = W_k^{\mathrm{BP}} - \eta_k G_k \tag{33}$$

where W_k^{BP} and G_k are the weight and the current gradient matrices, respectively and η_k is learning rate.

Levenberg-Marquardt (LM) [27] algorithm was designed to approach second-order training speed without having to compute the Hessian matrix. In the LM algorithm the weights updating is achieved as follows:

$$W_{k+1}^{\mathrm{BP}} = W_k^{\mathrm{BP}} - [J^{\mathrm{T}} J + \mu I]^{-1} J^{\mathrm{T}} E \tag{34}$$

where $\boldsymbol{J}$ is the Jacobian matrix that contains first derivatives of the network errors with respect to the weights; E is a vector of network errors; μ is a correction factor.

One of the techniques used to prevent overfitting is regularization [26] in which the performance function of the network is modified by adding a term that consists of the mean of the sum of squares of the network weights as:

$$mse_{\mathrm{reg}} = \gamma\left(\frac{1}{m}\sum_{i=1}^{m} E_i^2\right) + \frac{(1-\gamma)}{nw}\sum_{j=1}^{nw} (W_j^{BP})^2 \tag{35}$$

where γ and nw are the performance ratio and number of network weights, respectively; m is the size of E_i.

4.3 Prediction of seismic responses

NN models are trained to predict the structural seismic responses for implementation of MCS spending a reasonable amount of time. The input and output vectors of the NN models are represented for RC frames by Eqs. (16) and (21) and for steel frames by Eqs. (17) and (21), respectively. The topology of NN models trained to predict the responses of RC and steel frames are shown in Figures (2) and (3), respectively.

To evaluate the prediction accuracy of the trained NN models in testing mode, the absolute percentage error (*APE*) between the n_{ts} number of predicted and the actual responses and also mean absolute percentage error (*MAPE*) are computed as follows:

$$APE_j^i = \left| \frac{\theta_{\max}^i - \theta_{\max}^i}{\theta_{\max}^i} \right|_j \quad , \quad i = \text{IO, LS, CP} \quad , \quad j = 1, \ldots, n_{ts} \tag{36}$$

$$MAPE^i = \frac{1}{n_{ts}} \sum_{j=1}^{n_{ts}} \left(100\, APE_j^i\right) \quad , \quad i = \text{IO, LS, CP} \tag{37}$$

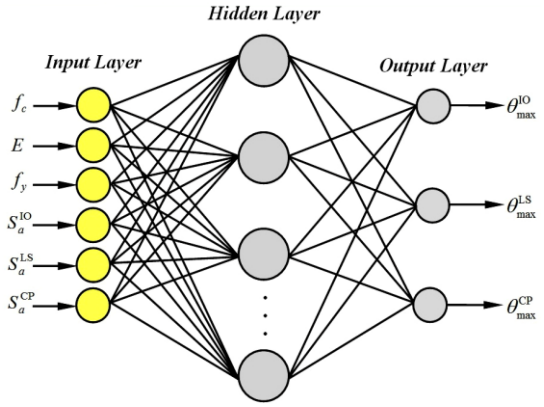

Figure 2. Topology of NN models for prediction of seismic responses of RC frames

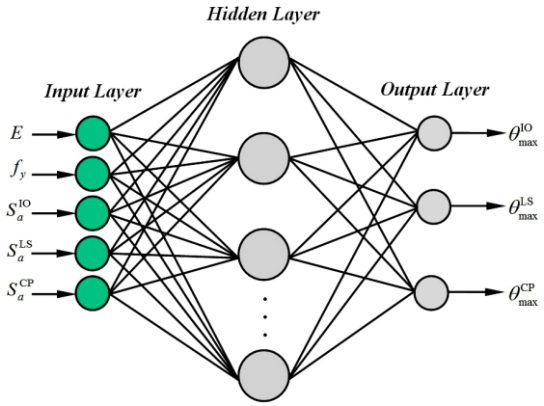

Figure 3. Topology of NN models for prediction of seismic responses of steel frames

5. NUMERICAL RESULTS

The numerical results of the present study are presented for RC and steel ordinery moment frames in this sections. The required computer programs for performing optimization processes are coded in MATLAB [28]. In addition, a personal Pentium IV 3.0 GHz is used for computer implementation.

For deterministic performance-based seismic design optimization of RC and steel moment frames the allowable values of inter-story drift in low-rise frame, for IO, LS and CP performance levels are taken according to HAZUS [29] provisions. These values in mid and high rise frames should be multiplied to 2/3 and 0.5, respectively.

In order to generate dataset for training NN models for RC and steel frames, Latin Hypercube Design (LHD) sampling [30] is employed.

5.1 RC frames

In order to illustrate the computational advantages of the proposed methodology in the case of RC frames, a three-bay, six-story and a four-bay, nine-story 2-D RC frames are considered. The geometry and element groups of the frames are shown in Figure 4.

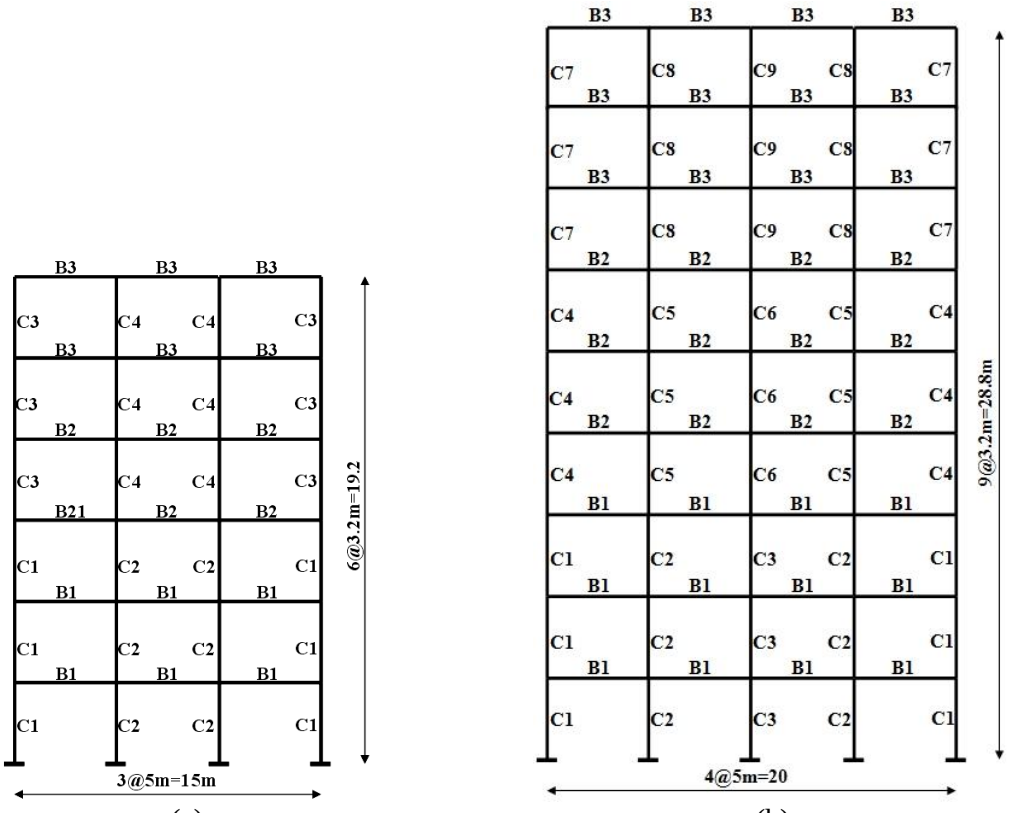

(a) (b)

Figure 4. Geometry and element groups for (a) three-bay, six-story and (b) four-bay, nine-story RC frames

Uniform gravity loads are considered on beams as a dead load DL = 25 kN/m and a live load LL = 10.0 kN/m. A semi-infinite set of member sizes and reinforcement arrangement for beams and columns is reduced by constructing databases in practical range. The databases information is sectional dimensions and number of reinforcing bars for the beams and columns as show in Tables 1 and 2, respectively.

Table 1: Cross section database for beams

Beam NO.	Width (cm)	Depth (cm)	Number of bars (D22)	
			Top	Bottom
1	30	45	2	2
2	30	45	3	2
⋮	⋮	⋮	⋮	⋮
496	45	90	9	8
497	45	90	9	9

Table 2: Cross section database for columns

Column NO.	Width (cm)	Depth (cm)	Number of bars (D25)
1	30	30	4
2	35	35	6
⋮	⋮	⋮	⋮
43	90	90	38
44	90	90	40

Median response spectra for three hazard levels [31] employed for RC frames are shown in Figure 5.

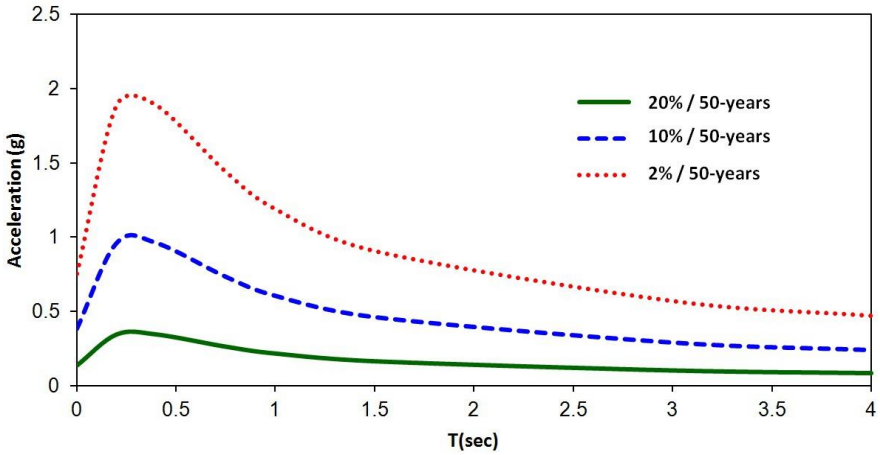

Figure 5. Median response spectra for three hazard levels [31]

In the RC frame examples deterministic parameters are as follows: ε_0=0.002, f_u=0.0, ε_u=0.005 and H=0.01. The properties, probability density function, mean value and standard deviation of each random parameter are given in Table 3.

Table 3: Properties of the random variables for RC frames

Random Variable	Probability density function	Mean value	Standard deviation
f_c	Normal	28 MPa	$0.1\,f_c$
E	Normal	200 GPa	$0.1E$
f_y	Normal	240 MPa	$0.1\,f_y$
S_a^{IO}	Lognormal	S_a^{IO} (Figure 5)	$0.15\,S_a^{\mathrm{IO}}$
S_a^{LS}	Lognormal	S_a^{LS} (Figure 5)	$0.15\,S_a^{\mathrm{LS}}$
S_a^{CP}	Lognormal	S_a^{CP} (Figure 5)	$0.15\,S_a^{\mathrm{CP}}$

5.1.1 Three-bay, six-story RC frame

The six-story RC frame is designed for optimal cost using BA meta-heuristic. In the optimization process a population of 30 bats is considered and the maximum number of generations is limited to 1000. During the optimization process the lateral inter-story drifts are checked at various performance levels as the design constraints. As this structure is a mid-rise frame, the allowable values of inter-story drift at IO, LS and CP levels are 0.66%, 2% and 5.33%, respectively. The results of optimization are given in Table 4.

Table 4: Results of optimization for three-bay, six-story RC frame

Element		Sectional dimensions		Reinforcements	
Type	Group	Width (cm)	Depth (cm)	Top	Bottom
Beam	B1	35	60	3-D22	3-D22
	B2	35	55	4-D22	4-D22
	B3	30	55	4-D22	3-D22
Column	C1	50	50	12-D25	
	C2	50	50	12-D25	
	C3	45	45	12-D25	
	C4	40	40	8-D25	
Frame cost (f_R)			33364 $		

Inter-story drift profiles of the optimum design are shown in Figure 6.

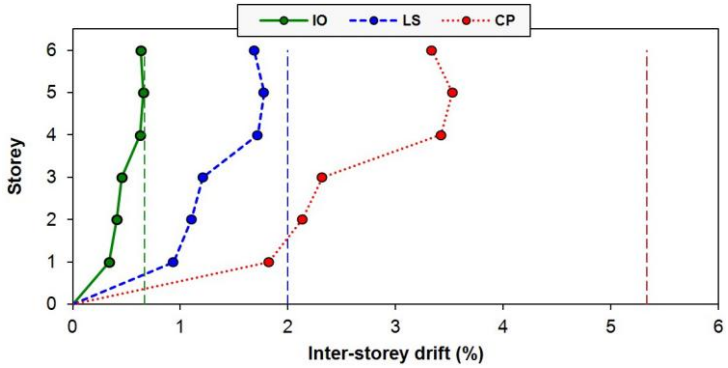

Figure 6. Inter-story drift profiles of the optimum six-story RC frame at performance levels

The vertical dashed lines denote drift limits for performance levels. It can observe that optimum solution is feasible and the constraint of IO level dominates the design.

In order to assess the seismic reliability of the optimum six-story RC frame, a database of random parameters should be generated. In this case, 8000 random vectors, i.e. $I_{NN,R}$, are selected and the resulted structures are analyzed using nonlinear pushover analysis and the maximum inter-story drifts, i.e. O_{NN}, are saved. The generated data is divided into training and testing sets including 7500 and 500 samples, respectively. RBF and BP models are trained and the results reveal that the computational performance of BP is very better than that of the RBF model. Thus, only the results of BP model are presented in this example. Various numbers of hidden layer neurons are examined for BP model and the best accuracy is achieved using 15 ones. Figure 7 shows the *APE* of the predicted θ_{max}^{IO}, θ_{max}^{LS} and θ_{max}^{CP}.

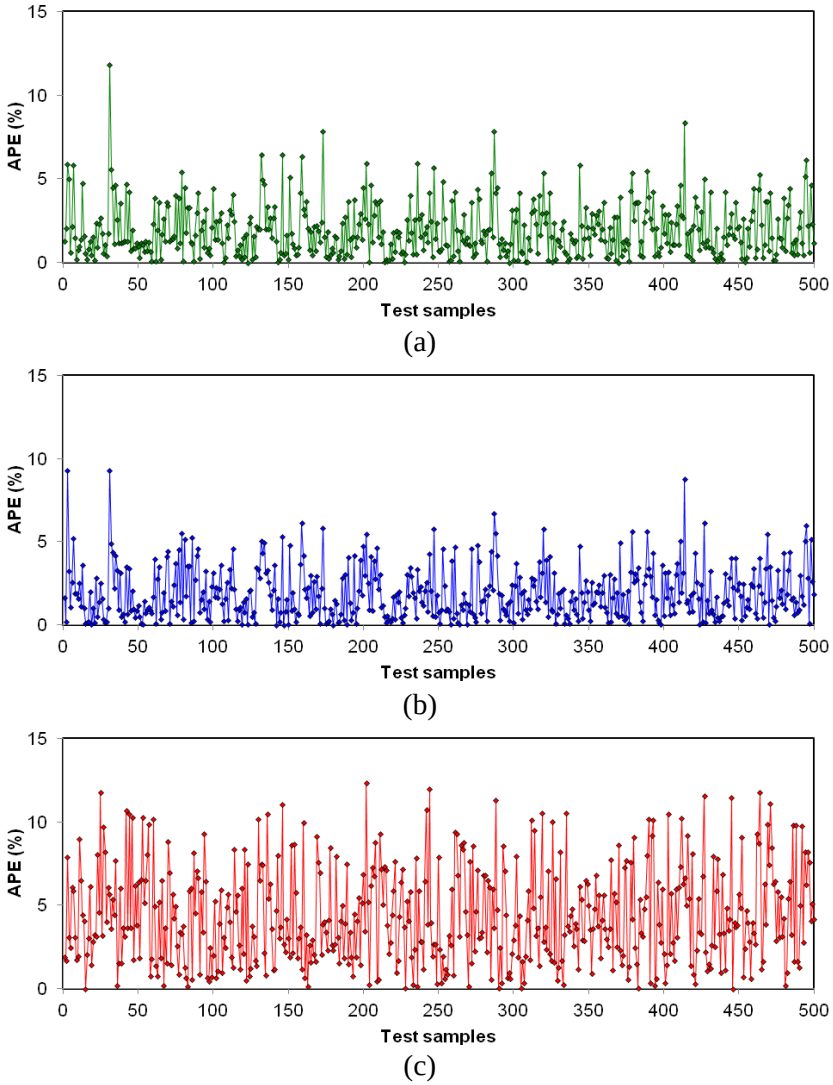

Figure 7. *APE* of the predicted θ_{max}^{IO}, θ_{max}^{LS} and θ_{max}^{CP} by BP for the optimum six-story RC frame

The *MAPE*s of the predicted $\theta_{\max}^{IO}$, $\theta_{\max}^{LS}$ and $\theta_{\max}^{CP}$ are respectively equal to 1.9319%, 1.8902% and 4.3626%. These results demonstrate the good accuracy of the trained BP for predicting the seismic responses of the structure. The trained BP model is effectively employed to implement MCS. In this case, 10^7 vectors of $I_{NN,R}$ are generated and their corresponding O_{NN} are predicted by the trained BP model. The values of Pf_E are calculated using Eqs. (29) and (32) for various performance levels. These values are shown in Figure 8 for various numbers of samples.

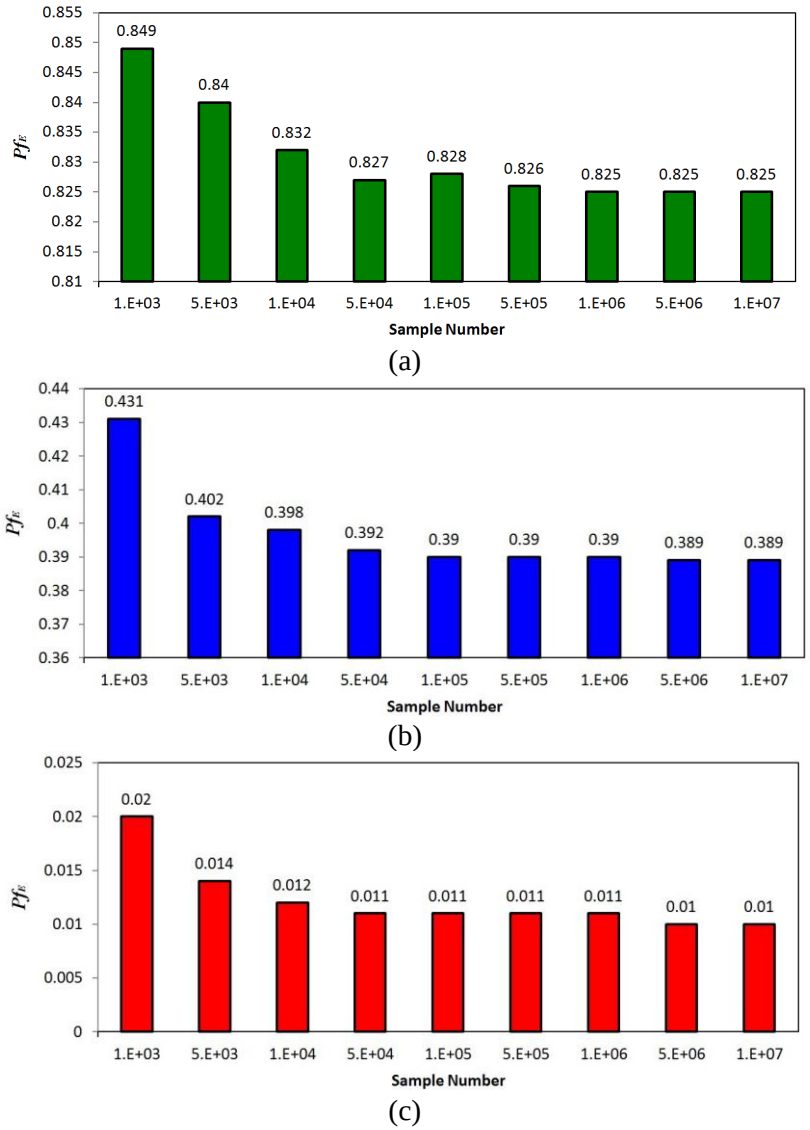

Figure 8. Total exceedence probability of limit state functions for the optimum six-story RC frame at (a) IO, (b) LS and (c) CP performance levels

These results indicate that the optimum six-story RC frame is highly vulnerable against the existing uncertainties at IO and LS performance levels. The results of Figure 8 reveal

that for all performance levels, the difference between Pf_E values obtained by 5×10^4 and 10^7 samples is trivial. It is clear that for seek of efficiency in terms of computational cost the application of 5×10^4 samples is the best choice.

5.1.2 Four-bay, nine-story RC frame

The BA is used to find performance-based optimal seismic design of the nine-story RC frame. The number of bats and the maximum number of generations during optimization process are 30 and 10000, respectively. This structure is considered as a high-rise frame and the allowable inter-story drift at IO, LS and CP levels are 0.5%, 1.5% and 4%, respectively. Optimization results are given in Table 5.

Table 5: Results of optimization for four-bay nine-story RC frame

Element		Sectional dimensions		Reinforcements	
Type	Group	Width (cm)	Depth (cm)	Top	Bottom
Beam	B1	40	60	5-D22	4-D22
	B2	40	60	3-D22	3-D22
	B3	30	50	4-D22	4-D22
Column	C1	60	60	16-D25	
	C2	60	60	16-D25	
	C3	55	55	14-D25	
	C4	55	55	14-D25	
	C5	50	50	12-D25	
	C6	45	45	10-D25	
	C7	45	45	10-D25	
	C8	45	45	10-D25	
	C9	45	45	10-D25	
Frame cost (f_R)				70315 $	

Inter-story drift profiles of the optimum design at various performance levels are shown in Figure 9.

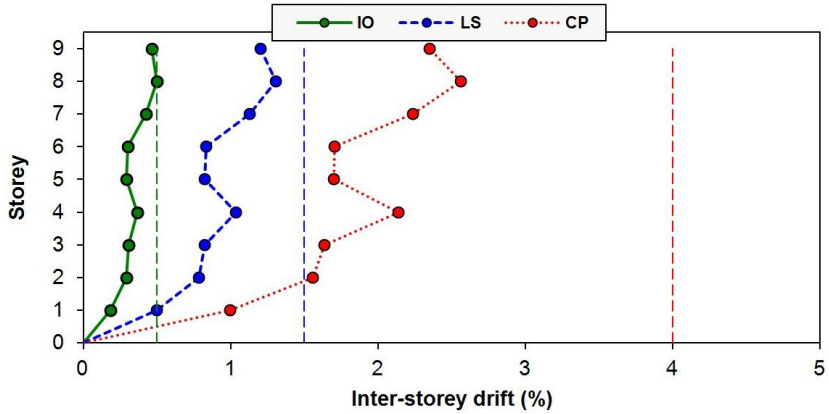

Figure 9. Inter-story drift profiles of the optimum nine-story RC frame at performance levels

The vertical dashed lines denote drift limits for performance levels. The results imply feasibility of optimum solution. It is observed again that the constraint associated with IO level dominates the design.

For assessing the seismic reliability of the optimum nine-story RC frame, a database of random vectors $I_{NN,R}$ and their corresponding O_{NN} including 12000 samples is generated and 11500 ones are used for training and 500 ones are employed for testing the NN models. As well as the first example, RBF and BP models are trained and the results demonstrate the superiority of BP to the RBF model. Therefore, in this example only the results based on application of BP model are presented.

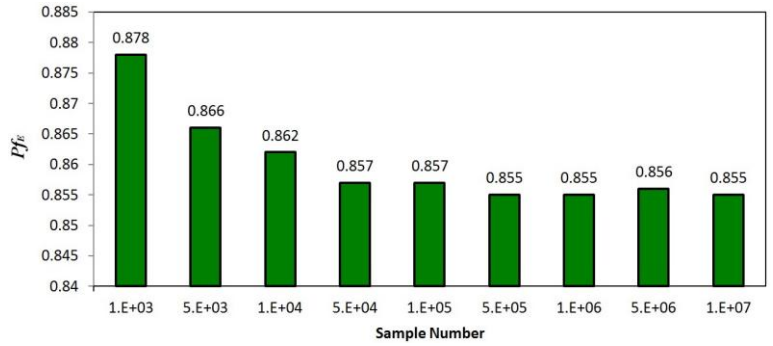

(a)

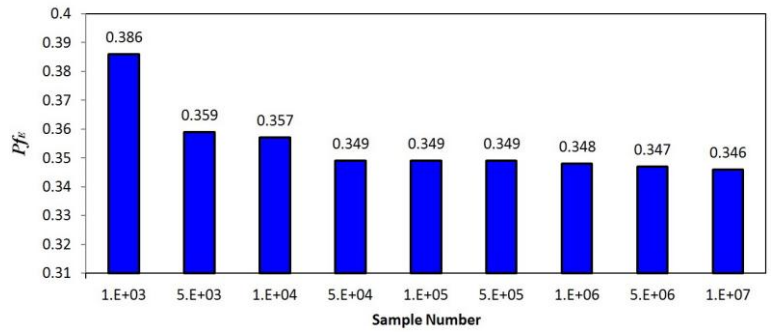

(b)

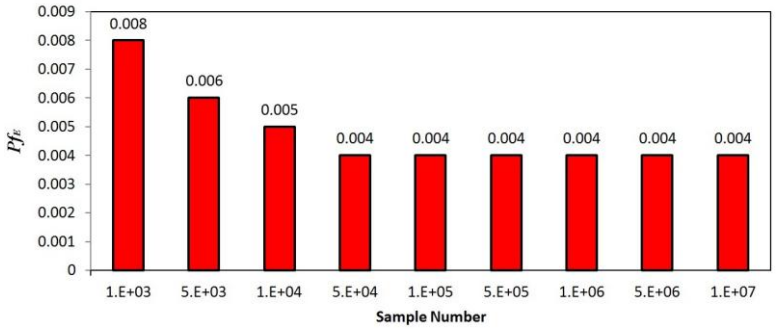

(c)

Figure 10. Total exceedence probability of limit state functions for the optimum nine-story RC frame at (a) IO, (b) LS and (c) CP performance levels

The numerical results indicate that the best results of BP model are obtained when 15 neurons are set in the hidden layer. The *MAPE*s of the predicted $\theta_{\max}^{IO}$, $\theta_{\max}^{LS}$ and $\theta_{\max}^{CP}$ are respectively equal to 2.2304%, 2.2393% and 4.5951%. These results demonstrate the good accuracy of the trained BP model. To implement MCS, 10^7 vectors of $I_{NN,R}$ are generated and their corresponding O_{NN} are predicted by the trained BP model. The values of Pf_E are calculated for various performance levels. These values are given in Figure 10.

Total exceedence probability of limit state functions for the optimum nine-story RC frame at IO, LS and CP performance levels are 0.855, 0.346 and 0.004, respectively. These obtained results imply the high vulnerability of the optimum nine-story RC frame against the existing uncertainties at IO and LS performance levels. The results of Figure 10 reveal that for all performance levels, the difference between Pf_E values obtained by 5×10^4 and 10^7 samples is trivial.

5.2 Steel frames

Two steel frame examples are presented to illustrate the computational performance of the proposed methodology. These examples include a two-bay, three-story and a three-bay, ten-story 2-D steel frames as shown in Figure 11.

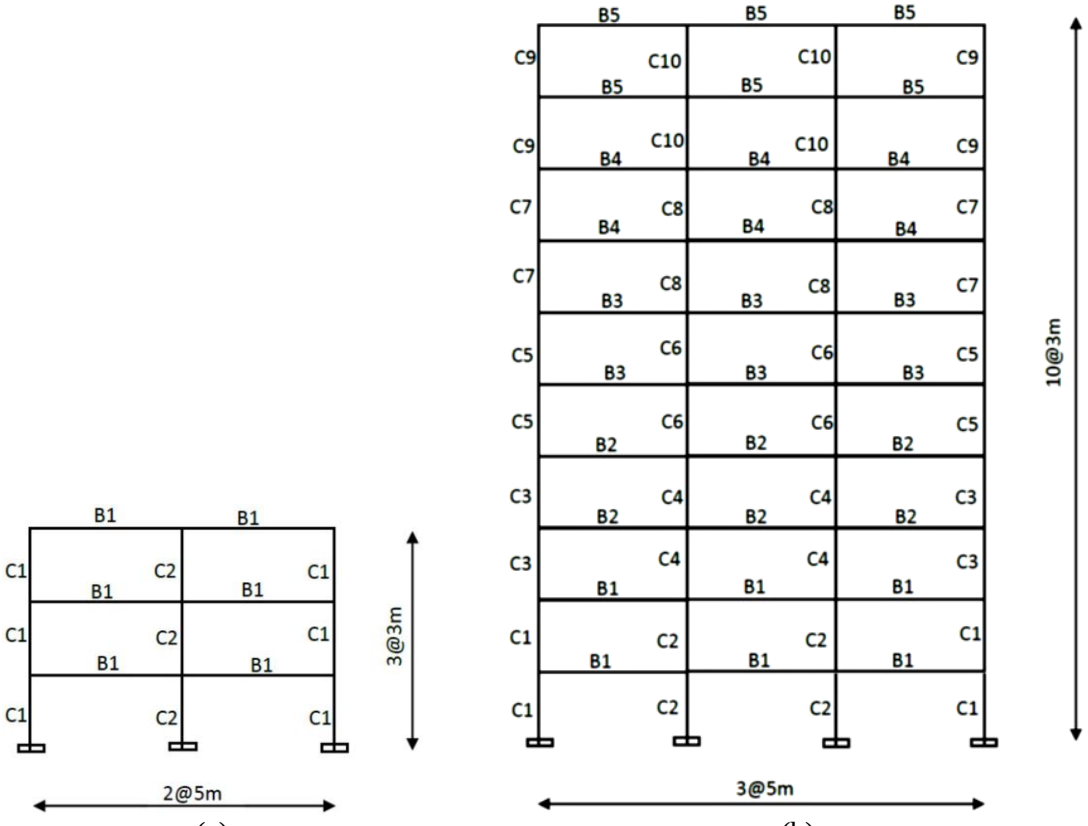

Figure 11. Geometry and element groups for (a) two-bay, three-story and (b) three-bay, ten-story steel frames

Uniform gravity loads are considered on beams as a dead load *DL* = 25 kN/m and a live load *LL* = 10.0 kN/m. In the present study, design variables of steel frames are selected from W-shaped sections found in the AISC [21] design manual.

The spectral acceleration S_a^i can be calculated for each design spectrum *i* as follows:

$$S_a^i = \begin{cases} F_a S_s^i (0.4 + 3T/T_0) & \text{if } 0 < T \le 0.2T_0^i \\ F_a S_s^i & \text{if } 0.2T_0^i < T \le T_0^i \\ F_v S_1^i / T & \text{if } T > T_0^i \end{cases}, \quad i = \text{IO, LS, CP} \tag{39}$$

$$T_0^i = \frac{F_v S_1^i}{F_a S_s^i} \tag{40}$$

where *T* is the elastic fundamental period of the structure, which is computed here from structural modal analysis; S_s^i and S_1^i are the short-period and the first sec.-period response acceleration parameters, respectively; T_0^i is the period at which the constant acceleration and constant velocity regions of the response spectrum intersect; F_a and F_v are the site coefficient determined respectively based on the site class and the values of the response acceleration parameters S_s^i and S_1^i, according to Table 6 [32].

Table 6: Performance level site parameters for site class of D

Performance Level	Hazard Level	S_s (*g*)	S_1 (*g*)	F_a	F_v
IO	20% / 50-years	0.658	0.198	1.27	2.00
LS	10% / 50-years	0.794	0.237	1.18	1.92
CP	2% / 50-years	1.150	0.346	1.04	1.70

In the steel frame examples deterministic parameter is *H*=0.03. The properties, probability density function, mean value and standard deviation of each random parameter are given in Table 7.

Table 7: Properties of the random variables for steel frames

Random Variable	Probability density function	Mean value	Standard deviation
E	Normal	210 GPa	$0.1E$
f_y	Normal	240 MPa	$0.1\, f_y$
S_a^{IO}	Lognormal	S_a^{IO} (Eq. (38))	$0.1\, S_a^{IO}$
S_a^{LS}	Lognormal	S_a^{LS} (Eq. (38))	$0.1\, S_a^{LS}$
S_a^{CP}	Lognormal	S_a^{CP} (Eq. (38))	$0.1\, S_a^{CP}$

5.2.1 Two-bay, three-story steel frame

The three-story steel frame is designed for optimal weight using BA meta-heuristic. In the

optimization process a population of 40 bats is considered and the maximum number of generations is limited to 300. During the optimization process the lateral inter-story drifts are checked at various performance levels as the design constraints. As this structure is a low-rise frame, the allowable values of inter-story drift at IO, LS and CP levels are 1.2%, 3% and 8%, respectively. The results of optimization are given in Table 8.

Table 8. Results of optimization for two-bay three-story steel frame

Design variables	Optimal sections
C1	W16×26
C2	W18×40
B1	W16×26
Weight (f_S)	2404.83 kg

Inter-story drift profiles of the optimum design are shown in Figure 12 for performance levels. The vertical dashed lines denote drift limits for performance levels. It can be observed that optimum solution is feasible and the constraint associated with IO level dominates the design.

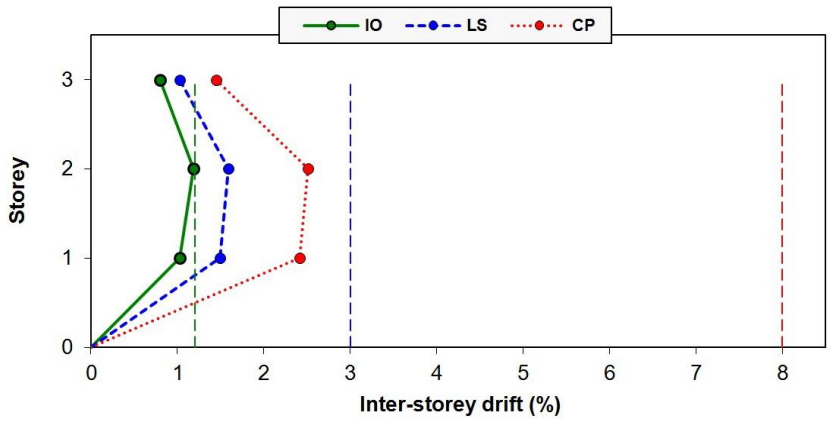

Figure 12. Inter-story drift profiles of the optimum three-story steel frame at performance levels

For performing seismic reliability analysis of the optimum three-story steel frame, a database including 10000 samples is generated. From the generated database 9000 and 1000 samples are employed for training and testing the NN models, respectively. As well as the RC frame example, RBF and BP models are trained and the results demonstrate the superiority of BP to the RBF model. Thus, in this example only the results of BP model are presented. The numerical results indicate that the best results of BP model are obtained when 5 neurons are set in hidden layer. The *MAPE*s of the predicted $\theta_{\max}^{\mathrm{IO}}$, $\theta_{\max}^{\mathrm{LS}}$ and $\theta_{\max}^{\mathrm{CP}}$ are respectively equal to 0.0043%, 0.1734% and 0.0994%. These results demonstrate the excellent accuracy of the trained BP model. To implement MCS, 10^7 vectors of $I_{\mathrm{NN,S}}$ are generated and their corresponding O_{NN} are evaluated by the BP model. The values of Pf_E are calculated for various performance levels and it is observed that for LS and CP performance

levels Pf_E =0. The values of Pf_E are given in Figure 13 for IO performance level.

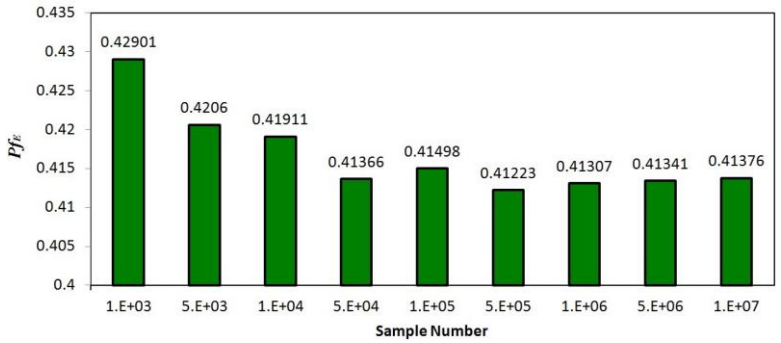

Figure 13. Total exceedence probability of limit state functions for the optimum three-story steel frame at IO performance level

It is clear that the optimum three-story steel frame is highly vulnerable against the existing uncertainties at IO level. The results of Figure 13 show that the difference between Pf_E values obtained by 5×10^4 and 10^7 samples is also trivial.

5.2.2 Three-bay, ten-story steel frame

The ten-story steel frame is designed for optimal weight using BA meta-heuristic. In the optimization process a population of 40 bats is considered and the maximum number of generations is limited to 500. The limits on the lateral inter-story drift at various performance levels are considered as the design constraints of this example. The results of optimization are given in Table 9.

Table 9. Results of optimization for three-bay ten-story steel frame

Design variables	Optimal sections
1	W21×55
2	W21×48
3	W24×55
4	W21×44
5	W21×44
6	W24×55
7	W30×99
8	W24×55
9	W21×55
10	W27×94
11	W21×55
12	W30×90
13	W16×36
14	W16×26
15	W16×26
Weight (f_S)	21033.91 kg

As well as the previous examples, in this example also the constraint associated with IO level dominates the design.

A database including 10000 samples is generated and from the generated database 9000 and 1000 samples are employed for training and testing the NN models, respectively. RBF and BP models are trained and due to better accuracy of BP with 5 hidden layer neurons, only the results of this model are discussed. The *MAPE*s of the predicted $\theta_{\max}^{\mathrm{IO}}$, $\theta_{\max}^{\mathrm{LS}}$ and $\theta_{\max}^{\mathrm{CP}}$ are respectively equal to 1.5033%, 1.6952% and 1.7395%. These results demonstrate good accuracy of the BP model. To implement MCS, 10^7 vectors of $I_{\mathrm{NN,S}}$ are generated and the BP model is employed to predict their corresponding O_{NN}. The values of Pf_E are calculated for various performance levels and it is observed that for LS and CP levels Pf_E =0. The values of Pf_E are given in Figure 14 for IO level.

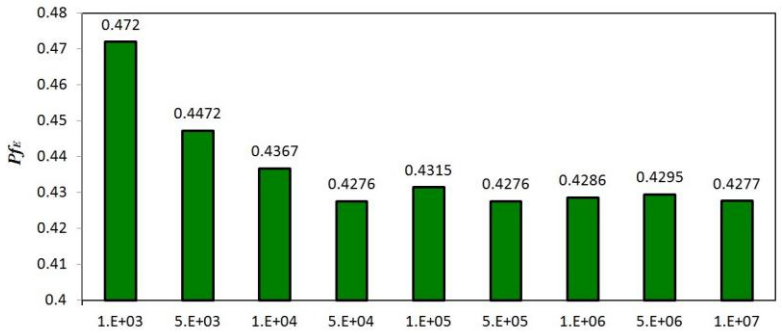

Figure 14. Total exceedence probability of limit state functions for the optimum ten-story steel frame at IO performance level

It is clear that the optimum ten-story steel frame is highly vulnerable against the uncertainties at IO level. The results of Figure 14 show again that the difference between Pf_E values obtained by 5×10^4 and 10^7 samples is trivial.

6. CONCLUSIONS

The main aim of the present paper is to assess the seismic reliability of performance-based optimally seismic designed RC and steel moment frames by a combination of MCS and NN models. In order to achieve this purpose, two RC structures including six and nine story frames and two steel structures including three and ten story frames are optimized based on PBD criteria using BA meta-heuristic. During the optimization process the lateral inter-story drifts are checked at IO, LS and CP performance levels as the design constraints. For all examples, the constraint associated with IO level dominates the design. In order to assess the seismic reliability of the optimum structures, a database is generated in the case of each example. The generated data is divided into training and testing sets. RBF and BP models are trained and the results reveal that for all examples the computational performance of BP is better than that of the RBF model. The trained BP model is effectively employed to implement MCS. In this case, 10^7 input vectors are generated and their corresponding

outputs are predicted by the trained BP model. These results indicate that the optimum RC frames are highly vulnerable against the existing uncertainties at IO and LS performance levels with the mean exceedence probability of about 0.8 and 0.3, respectively. For the optimum steel frames, the mean exceedence probability for IO level is about 0.4 while good safety is observed for these structures at LS and CP performance levels. The results indicate that the optimum performance-based RC and steel moment frames are highly vulnerable against existing uncertainties of structural capacity and seismic demands. Therefore, implementation of seismic reliability-based optimization for these structures is necessary to have seismically reliable and safe structures.

REFERENCES

1. FEMA-356. Prestandard and commentary for the seismic rehabilitation of buildings. Washington DC: Federal Emergency Management Agency, SAC Joint Venture; 2000.
2. SEAOC Vision 2000 Committee. Performance based seismic engineering of buildings. Sacramento, California, USA: Structural Engineers Association of California; 1995.
3. Applied Technology Council, ATC-40. Seismic evaluation and retrofit of concrete buildings. California Seismic Safety Commission; 1997.
4. Kwon OS, Elnashai A. The effect of material and ground motion uncertainty on the seismic vulnerability of RC structure, *Eng Struct*, 2006; **28**: 289–303.
5. Ramamoorthy SK, Gardoni P, Bracci JM. Probabilistic demand models and fragility curves for reinforced concrete frames, *J Struct Eng*, 2006; **132**: 1563–72.
6. Buratti N, Ferracuti B, Savoia M. Response surface with random factors for seismic fragility of reinforced concrete frames, *Struct Safe*, 2010; **32**: 42–51.
7. Moller O, Foschi RO, Quiroz LM, Rubinstein M. Structural optimization for performance-based design in earthquake engineering: applications of neural networks, *Struct Safe*, 2009; **31**: 490–9.
8. Moller O, Foschi RO, Rubinstein M, Quiroz LM. Seismic structural reliability using different nonlinear dynamic response surface approximations, *Struct Safe*, 2009; **31**: 432–42.
9. Khatibinia M, Fadaee MJ, Salajegheh J, Salajegheh E. Seismic reliability assessment of RC structures including soil–structure interaction using wavelet weighted least squares support vector machine, *Reliab Eng Syst Safe*, 2013; **110**: 22–33.
10. Lagaros ND, Plevris V, Papadrakakis M. Neurocomputing strategies for solving reliability-robust design optimization problems, *Eng Comput*, 2010; **27**: 819–40.
11. Shooman ML. Probabilistic reliability: an engineering approach. McGraw-Hill; 1968.
12. Yang XS. A new metaheuristic bat-inspired algorithm. *In: Gonzalez JR et al. (eds) Nature inspired cooperative strategies for optimization (NISCO 2010)*. *Studies in Computational Intelligence*, vol 284. Springer, Berlin, pp. 65–74, 2010.
13. Gandomi AH, Yang XS, Alavi AH, Talatahari S. Bat algorithm for constrained optimization tasks, *Neural Comput Appl*, DOI 10.1007/s00521-012-1028-9.
14. Fragiadakis M, Lagaros ND. An overview to structural seismic design optimisation frameworks, *Comput Struct*, 2011; **89**: 1155–65.

15. FEMA-440. Improvement of Nonlinear Static Seismic Analysis Procedure Federal Emergency Management Agency Washington, D.C., 2005.
16. McKenna F, Fenves GL. The OpenSees Command Language Manual (1.2. edn). PEER, 2001.
17. Gholizadeh S, Aligholizadeh V. Optimum design of reinforced concrete frames using bat meta-heuristic algorithm, *Int J Optim Civil Eng*, 2013; **3**: 483–97.
18. Gholizadeh S, Kamyab R, Dadashi H. Performance-based design optimization of steel moment frames, *Int J Optim Civil Eng*, 2013; **3**: 327–43.
19. Vanderplaats GN. *Numerical Optimization Techniques for Engineering Design: With Application*, McGraw-Hill, New York, 1984.
20. American Concrete Institute (ACI). Building code requirements for structural concrete and commentary. ACI 318–08, 2008.
21. Manual of steel construction. Load and resistance factor design, Chicago, IL: American Institute of Steel Construction, 2001.
22. Carbas S, Hasancebi O. Optimum design of steel space frames via bat inspired algorithm, *10th World Congress on Structural and Multidisciplinary Optimization*, Florida, USA, 2013.
23. Kent DC, Park R. Flexural members with confined concrete, *J Struct Div*, *ASCE*, 1997; **97**: 1969–90.
24. Gholizadeh S, Salajegheh J, Salajegheh E. An intelligent neural system for predicting structural response subject to earthquakes, *Adv Eng Softw*, 2009; **40**: 630−9.
25. Wasserman PD. Advanced methods in neural computing, New York: Prentice Hall Company, Van Nostrand Reinhold, 1993.
26. Hagan MT, Demuth HB, Beal MH. Neural network design, PWS Publishing Company, Boston, 1996.
27. Hagan MT, Menhaj M. Training feed-forward networks with the Marquardt algorithm, *IEEE Trans Neural Network*, 1999; **5**: 989−93.
28. The Language of Technical Computing, MATLAB. Math Works Inc, 2009.
29. FEMA-National Institute of Building Sciences, HAZUS-MH MR1, Multi-hazard Loss Estimation Methodology Earthquake Model, Washington, DC, 2003.
30. Mckay MD, Beckman RJ, Conover WJ. A comparison of three methods for selecting values on input variables in the analysis of output from a computer code, *Tech*, 1979; **21**: 439–45.
31. Webpage: http://iranhazard.mporg.ir/PSHA.aspx.
32. Kaveh A, Farahmand Azar B, Hadidi A, Rezazadeh Sorochi F, Talatahari S. Performance-based seismic design of steel frames using ant colony optimization, *J Constr Steel Res*, 2010; **66**: 566–74.